Enzymatic transformation of nonfood biomass to starch

Chun You[a,1], Hongge Chen[a,b,1], Suwan Myung[a,c], Noppadon Sathitsuksanoh[a,c], Hui Ma[d], Xiao-Zhou Zhang[a,d], Jianyong Li[e], and Y.-H. Percival Zhang[a,c,d,f,g,2]

[a]Biological Systems Engineering Department, [c]Institute for Critical Technology and Applied Science, and [e]Biochemistry Department, Virginia Polytechnic Institute and State University, Blacksburg, VA 24061; [b]College of Life Sciences, Henan Agricultural University, Zhengzhou 450002, China; [d]Gate Fuels, Inc., Blacksburg, VA 24060; [f]BioEnergy Science Center, Department of Energy, Oak Ridge, TN 37831; and [g]Cell Free Bioinnovations, Inc., Blacksburg, VA 24060

Edited* by Arnold L. Demain, Drew University, Madison, NJ, and approved March 27, 2013 (received for review February 5, 2013)

The global demand for food could double in another 40 y owing to growth in the population and food consumption per capita. To meet the world's future food and sustainability needs for biofuels and renewable materials, the production of starch-rich cereals and cellulose-rich bioenergy plants must grow substantially while minimizing agriculture's environmental footprint and conserving biodiversity. Here we demonstrate one-pot enzymatic conversion of pretreated biomass to starch through a nonnatural synthetic enzymatic pathway composed of endoglucanase, cellobiohydrolyase, cellobiose phosphorylase, and alpha-glucan phosphorylase originating from bacterial, fungal, and plant sources. A special polypeptide cap in potato alpha-glucan phosphorylase was essential to push a partially hydrolyzed intermediate of cellulose forward to the synthesis of amylose. Up to 30% of the anhydroglucose units in cellulose were converted to starch; the remaining cellulose was hydrolyzed to glucose suitable for ethanol production by yeast in the same bioreactor. Next-generation biorefineries based on simultaneous enzymatic biotransformation and microbial fermentation could address the food, biofuels, and environment trilemma.

bioeconomy | food and feed | synthetic amylose | in vitro synthetic biology | cell-free biomanufacturing

The continuing growth of the population and food consumption per capita means that the global demand for food could increase by 50–100% by 2050 (1, 2), and ∼30% of the world's agricultural land and 70% of the world's fresh water withdrawals are being used for the production of food and feed to support 7 billion people (3, 4). Starch is the most important dietary component because it accounts for more than half of the consumed carbohydrates, which provide 50–60% of the calories needed by humans. Starch is composed of polysaccharides consisting of a large number of glucose units joined together primarily by alpha-1,4-glycosidic bonds and alpha-1,6-glycosidic bonds. Linear-chain amylose is more valuable than branched amylopectin because it can be used as a precursor for making high-quality transparent, flexible, low-oxygen-diffusion plastic sheets and films (5, 6); tailored functional food or additives for lowering the risk of serious noninfectious diseases (e.g., diabetes and obesity) (7, 8); and a potential high-density hydrogen carrier (9–11). Also, it is easy to convert linear amylose to branched amylopectin by using alpha-glucan–branching glycosyltransferase (12).

Cellulose, a linear glucan linked by beta-1,4-glycosidic bonds, is the supporting material of plant cell walls and the most abundant carbohydrate on Earth. The annual resource of cellulosic materials is ∼40 times greater than the starch produced by crops cultivated for food and feed. In addition, (perennial) cellulosic plants and dedicated bioenergy crops can grow on low-quality land, even on marginal land, and require fewer inputs such as fertilizers, herbicides, pesticides, and water, whereas annual high-productivity starch-rich crops require high-quality arable land, enough water, and high inputs (4, 13). Every ton of cereals harvested is usually accompanied by the production of two to three tons of cellulose-rich crop residues, most of which are burned or wasted rather than used for cellulosic biorefineries (4, 14).

The cost-effective transformation of nonfood cellulose to starch could revolutionize agriculture and reshape the bioeconomy, while maintaining biodiversity, minimizing agriculture's environmental footprint, and conserving fresh water (4, 15). This transformation would not only promote the cultivation of plants chosen for rapid growth rather than those optimized for starch production, but it would also efficiently use marginal land for the production of the biomass required to meet the increasing needs for biofuels and renewable materials (4, 16–18). Some cellulolytic microorganisms can accumulate microbial glycogen, but maximum glycogen yields are very low, for example, 2–4% (wt/wt) (19, 20). These low yields are due mainly to the fact that the majority of the carbon source is used for the synthesis of cell mass rather than of glycogen (19, 20). Researchers in the field of synthetic biology wish to develop high-yield, glycogen-accumulating cellulolytic microorganisms, but this task remains challenging because of their complicated cellular systems (17).

The cost-effective release of soluble fermentative sugars from cellulosic materials through enzymatic hydrolysis is essential in second-generation cellulosic biorefineries (21). In enzymatic hydrolysis, a soluble hydrolytic intermediate, cellobiose, a major product of cellobiohydrolases (CBHs; EC 3.2.1.91), is rapidly hydrolyzed to glucose by adding excessive beta-glucosidase (BG) to prevent product inhibition of CBHs and endoglucanases (EGs; EC 3.2.1.4). Glucose cannot be used directly for the synthesis of starch because of the required energy input for the formation of alpha-1,4-glycosidic bonds among the glucose units. For example, in vivo starch and glycogen are usually synthesized from activated precursors such as ADP-glucose in plants and UDP-glucose in animals (22).

In vitro synthetic biology enables the rapid construction of nonnatural enzymatic pathways and often has more appealing advantages, such as higher product yields, faster reaction rates, and better tolerances to toxic compounds, than those mediated by living organisms (10, 23–31). Here we design a cell-free biosystem composed of a synthetic enzymatic pathway that can transform solid cellulose into amylose in high yields. This pathway is composed of several extracellular hydrolytic enzymes and two intracellular enzymes. These enzymes are separated by the cellular membrane in natural systems. A bioprocess called simultaneous enzymatic biotransformation and microbial fermentation (SEBF)

Author contributions: C.Y., H.C., and Y.-H.P.Z. designed research; C.Y. and H.C. performed research; S.M., H.M., and X.-Z.Z. contributed new reagents/analytic tools; C.Y., H.C., N.S., J.L., and Y.-H.P.Z. analyzed data; and H.C. and Y.-H.P.Z. wrote the paper.

Conflict of interest statement: The authors have filed a provisional patent disclosure (Zhang Y-HP, Chen H. Conversion of cellulose to starch through an in vitro synthetic enzymatic pathway. Filed on December 17, 2012.).

*This Direct Submission article had a prearranged editor.

[1]C.Y. and H.C. contributed equally to this work.

[2]To whom correspondence should be addressed. E-mail: ypzhang@vt.edu.

This article contains supporting information online at www.pnas.org/lookup/suppl/doi:10.1073/pnas.1302420110/-/DCSupplemental.

was developed to coproduce amylose, ethanol, and single-cell protein in one bioreactor to meet different needs from (tailored) food and feed to renewable materials and biofuels.

Results

We designed an enzymatic pathway that can transform cellulose to amylose (Fig. 1*A*). This pathway has two modules: (*i*) partial hydrolysis of cellulose to cellobiose by optimizing the CBH and EG composition and ratio and (*ii*) amylose synthesis using a glycoside hydrolase family 9 cellobiose phosphorylase (CBP; EC 2.4.1.20) and a glycosyltransferase family 35 alpha-glucan phosphorylase (αGP; EC 2.4.1.1). In this system, CBP reversibly converts cellobiose to glucose-1-phosphate (G-1-P) and glucose in the presence of phosphate ions, the special αGP adds one glucose unit from G-1-P at the nonreducing end of amylose or maltodextrins, and phosphate ions are recycled to maintain nearly constant pH and phosphate levels (Fig. 1*A*).

Five cellulase components were used to optimize the cellulose degradation and hydrolysis product distribution of the pretreated Avicel regenerated amorphous cellulose (RAC). These cellulases included two EGs, glycoside hydrolase family 5 *Bacillus subtilis* endoglucanase (BsCel5) and *Trichoderma* spp. endoglucanase II (TrCel5A), and three CBHs, family 7 *Trichoderma* spp. cellobiohydrolase (TrCel7A), family 9 *Clostridium phytofermentans* cellobiohydrolase (CpCel9), and family 48 *C. phytofermentans* cellobiohydrolase (CpCel48) (32). All recombinant enzymes were produced in *Escherichia coli* BL21 (DE3) and purified to homogeneity (Fig. S1*A*), except for the *Trichoderma* enzymes, which were purchased. The sole cellulase component did not efficiently hydrolyze pretreated cellulose, whereas combinations of an EG and a CBH led to higher cellulose degradation (Table S1). However, the distribution of soluble products from glucose to cellotriose varied greatly, depending on the enzyme combination (Fig. S1*B* and Table S2). Based on the cellobiose yield and the cellulose degradation (Fig. S1*C* and Table S1), the best cellulase combination was bacterial BsCel5 and fungal TrCel7A.

A combination of the *Clostridium thermocellum* CBP (33, 34) and the special αGP was used for the synthesis of amylose from cellobiose. Although building blocks for in vitro synthetic biology projects are highly interchangeable (28), we found that whether amylose was synthesized from cellobiose depended on the choice of αGP. Three αGPs, one from potato (*Solanum tuberosum*) and two thermophilic bacteria, *C. thermocellum* (35) and *Thermotoga maritima*, were tested. Among them, only the potato αPG (PGP) was able to drive the reversible reactions mediated by CBP and αGP toward the synthesis of amylose.

The one-pot transformation of RAC to amylose was implemented by four enzymes, BsCel5, TrCel5A, CBP, and PGP, in 0.5 mL of reaction volume (Fig. 1*B*). The RAC slurry (Fig. 1*B*, tube 1) was completely hydrolyzed and then converted into amylose (tube 3). The synthetic amylose exhibited a deep blue color in the presence of iodine (tube 4), whereas the negative control (cellulose/iodine) was yellow (tube 2). The soluble amylose was precipitated by the addition of ethanol (tube 5). The amylose yield was 14.4% (wt/wt) (i.e., 0.144 g of amylose per gram of cellulose), and the number-average degree of polymerization was ~150. The addition of glucose oxidase to remove glucose, a strong inhibitor of CBP, resulted in a yield increase to 30.0% (wt/wt) (tube 6) (Fig. S2). However, the use of glucose oxidase resulted in a net loss in glucose (36). The number-average of degree of polymerization varied from 140 to 250, depending on the amount of maltotetraose added and cellobiose availability

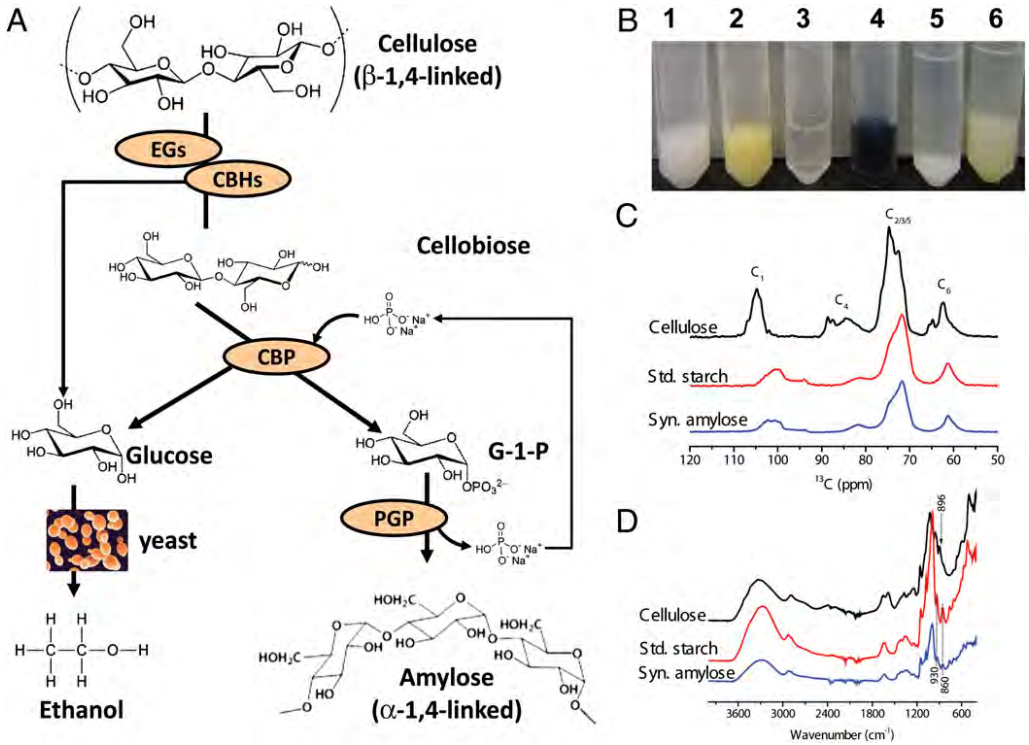

Fig. 1. The enzymatic cellulose hydrolysis using endoglucanases (EGs), cellobiohydrolases (CBHs) and beta-glucosidase (BG) in cellulosic ethanol biorefinery versus the synthetic cellulose-to-amylose pathway supplemented with cellobiose phosphorylase (CBP) and potato alpha-glucan phosphorylase (PGP) (*A*). Characterization of synthetic starch by iodine dyeing (*B*), CP/MAS ^{13}C-NMR (*C*), and FTIR (*D*). Tube 1, cellulose-suspended solution; tube 2, cellulose solution plus iodine/potassium iodide; tube 3, water-soluble synthetic starch solution made from cellulose mediated by the four- enzyme mixture; tube 4, synthetic starch solution plus iodine/potassium iodide; tube 5: precipitated starch by ethanol addition; and tube 6, precipitated starch when the mixture was supplemented with glucose oxidase.

(Table S3), where maltotetraose was used as the primer for amylose synthesis catalyzed by PGP. Synthetic amylose was validated by the hydrolysis of glucoamylase, followed by a hexokinase-based glucose assay, cross-polarization magic-angle spinning ^{13}C-NMR (Fig. 1*C*), and FTIR (Fig. 1*D*). Cellulose exhibited completely different C1 and C4 peaks compared with the amylose standard and synthetic amylose (Fig. 1*C*). In the FTIR (Fig. 1*D*), the bands at 930 and 860 cm^{-1} are typical signatures of alpha-1,4–linked amylose. The band at 896 cm^{-1}, a signature of beta-1,4–linked cellulose, was not observed in the starch samples. The above evidence suggests that amylose was synthesized from cellulose.

Among the three tested αGP proteins, only PGP can synthesize amylose from cellobiose. A Basic Local Alignment Search Tool search of the PGP sequence against protein databases of various model species from bacteria to humans identified the related proteins. Comparison of these sequences indicated that the residues involved in substrate binding and catalysis were fairly conserved among all αGP sequences. Phylogenetic analysis suggests that these αGP enzymes evolved from a common ancestor, and the enzymes from the original plant were evolutionally conserved (Fig. 2). The *C. thermocellum* αGP and the *T. maritima* αGP were highly similar to each other but were far different from PGP. We built homology structure models for all αGPs and observed that PGP and four other plant αGPs (*Ipomoea batatas*, *Spinacia oleracea*, *Oryza sativa*, and *Triticum aestivum*) had a special cap on their catalytic site that was absent in all bacterial αGPs and other plant αGPs (e.g., *Zea mays* and *Arabidopsis thaliana*). Fig. 3*A* illustrates the major structural difference between PGP and *T. maritima* αGP. Therefore, we hypothesized that the polypeptide cap on the catalytic site of PGP was responsible for driving low-concentration G-1-P toward the synthesis of amylose. We designed two PGP mutants; one had a part of the polypeptide cap removed and the other did not have the cap at all (Fig. S3 and Tables S4 and S5). In the buffer containing cellobiose and CBP, the partially decapped PGP (PDC-PGP) had decreased amylose synthesis ability compared with wildtype (Fig. 3*B*, tube 2), whereas the completely decapped PGP (CDC-PGP) lost this ability completely (Fig. 3*B*, tube 3). The K_m and k_{cat} values of PGP, PDC-PGP, CDC-PGP, and *C. thermocellum* αGP are compared in Table 1. The removal of the cap of PGP decreased the k_{cat}/K_m values from 3.33 to 0.43 $mM^{-1}{\cdot}s^{-1}$ in the starch synthesis direction and from 0.55 to 0.06 $mM^{-1}{\cdot}s^{-1}$ in the starch degradation direction. Compared with the *C. thermocellum* αGP, PGP has a higher k_{cat}/K_m value in the synthesis direction and a lower k_{cat}/K_m in the degradation direction, suggesting that wild-type PGP has a preferred function for starch synthesis to degradation. Additionally, PGP has a lower activation energy for synthesis and a high activation energy for degradation. This result suggests the importance of identifying the correct building blocks for in vitro synthetic biology systems.

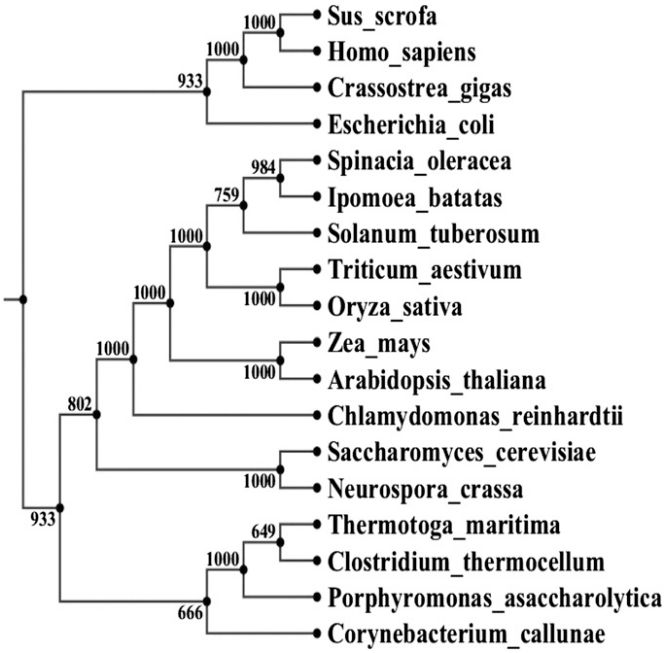

Fig. 2. A phylogenetic tree for the selected alpha-glucan phosphorylases.

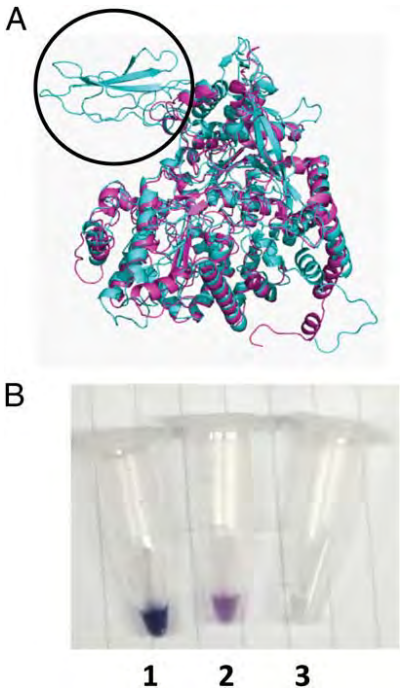

Fig. 3. Homology structure comparison between PGP (cyan) and *Thermotoga maritima* alpha-glucan phosphorylase (purple) (*A*) and photos of starch-synthesizing ability (*B*) from cellobiose mediated by CBP and wild-type PGP (tube 1), partially decapped PGP (tube 2), or completely decapped PGP (tube 3).

To achieve selective recycling of CBP and PGP from the enzymatic cellulose hydrolysate and fermentation broth, we also developed a simple enzyme purification and coimmobilization process using Avicel-containing nanomagnetic particles (A-NMPs) (Fig. 4). A-NMPs with a diameter of 400–600 nm were synthesized (Fig. 4*A*) according to the modified solvothermal synthesis method (37). Family 3 cellulose-binding module (CBM3)–containing proteins (e.g., CBM3-containing green fluorescent protein) can be bound tightly on the surface of A-NMPs because of the high-affinity adsorption of CBM3 on the surface of cellulose. The immobilized CBM3-containing enzyme or complex on A-NMPs can be easily separated from the aqueous solution using a magnetic field (Fig. 4*B*). We produced three recombinant proteins in *E. coli* BL21 (DE3): miniscaffoldin (38), CtDoc-LL-PGP, and CBP-RfDoc (Tables S4 and S5). The synthetic protein miniscaffoldin contained one CBM3, one cohesin module from CipA of *C. thermocellum*, one cohesin module from CbpA of *Clostridium cellulovorans*, and one cohesin module of ScaB from *Ruminococcus flavefaciens* in tandem (38). CtDoc-LL-PGP was composed of a *C. thermocellum* dockerin and PGP linked by a long linker. CBP-RfDoc was composed of *C. thermocellum* CBP and a *R. flavefaciens* dockerin. Because of the high-affinity interaction among cohesins and dockerins, the three proteins can be self-assembled as an enzyme complex (Fig. 4*C*). Therefore, we prepared the immobilized CBP–PGP complex on A-NMPs by mixing three cell extracts with

Table 1. Comparison of potato alpha-glucan phosphorylase and mutants and a thermophilic *C. thermocellum* alpha-glucan phosphorylase

	Amylose synthesis*				Amylose degradation†					
Name	k_{cat}, s^{-1}	K_m,‡ mM	k_{cat}/K_m, $mM^{-1}{\cdot}s^{-1}$	E_a,§ KJ/moL	k_{cat}, s^{-1}	K_m,‡ mM	k_{cat}/K_m, $mM^{-1}{\cdot}s^{-1}$	E_a,§ KJ/moL	k_{cat}/K_m ratio, syn/deg¶	E_a ratio, syn/deg¶
PGP	5.83 ± 0.34	1.76 ± 0.18	3.33	18.3	0.90 ± 0.11	1.64 ± 0.13	0.55	59.7	6.5	0.31
PDC-PGP	4.88 ± 0.27	1.92 ± 0.21	2.54	14.4	0.83 ± 0.09	2.20 ± 0.21	0.38	26.6	5.9	0.54
CDC-PGP	0.95 ± 0.11	2.22 ± 0.41	0.43	13.4	0.19 ± 0.04	3.11 ± 0.23	0.06	20.7	5.0	0.65
CthαGP	6.6 ± 0.3	1.9 ± 0.2	3.50	50.6	8.1 ± 0.2	0.39 ± 0.01	21.0	16.8	0.8	3.01

*The activities were assayed at 37 °C in a 100 mM Hepes buffer (pH 7.4) containing 10 mM Mg^{2+}, 20 mM G1P at maltodextrin (419672; Sigma; dextrose equivalent of 4.0–7.0) concentrations between 0.2 and 5 times their respective K_m values.
†The activities were assayed at 37 °C in a 100 mM Hepes buffer (pH 7.4) containing 10 mM Mg^{2+} and 20 mM inorganic phosphate at various maltodextrin concentrations between 0.2 and 5 times their respective K_m values.
‡The concentrations of maltodextrin were given as the molar concentration of the nonreducing ends.
§The Arrhenius plot was depicted as $\ln(k_{cat})$ versus 1/T (K) and the activation energy (E_a) was calculated from the slope of the plot.
¶Syn/deg means synthesis/degradation.

A-NMPs followed by magnetic separation (Figs. S4 and S5). The immobilized CBP–PGP enzyme complexes exhibited the same reaction rates as the noncomplexed CBP and PGP mixture (Fig. 4*D*), suggesting that this enzyme coimmobilization did not impair enzymatic activity.

We developed a bioprocess, SEBF, that can transform pretreated biomass to amylose, ethanol, and yeast as single-cell protein in one bioreactor (Fig. 1*A*). This process may be regarded as modified simultaneous saccharification and fermentation (SSF) in second-generation cellulosic biorefineries, where beta-glucosidase was replaced with immobilized CBP–PGP that can be easily recycled by a magnetic force. In the proof-of-concept SEBF experiment, we used a mixture of fungal TrCel7A, bacterial BsCel5, and CpCel48 (32) for hydrolyzing pretreated biomass, such as RAC, and diluted acid (DA)-pretreated and cellulose solvent- and organic solvent-based lignocellulose fractionation (COSLIF)-pretreated corn stover (39). In this system, nonused glucose units generated from the cellulases and CBP were assimilated by ethanol-producing

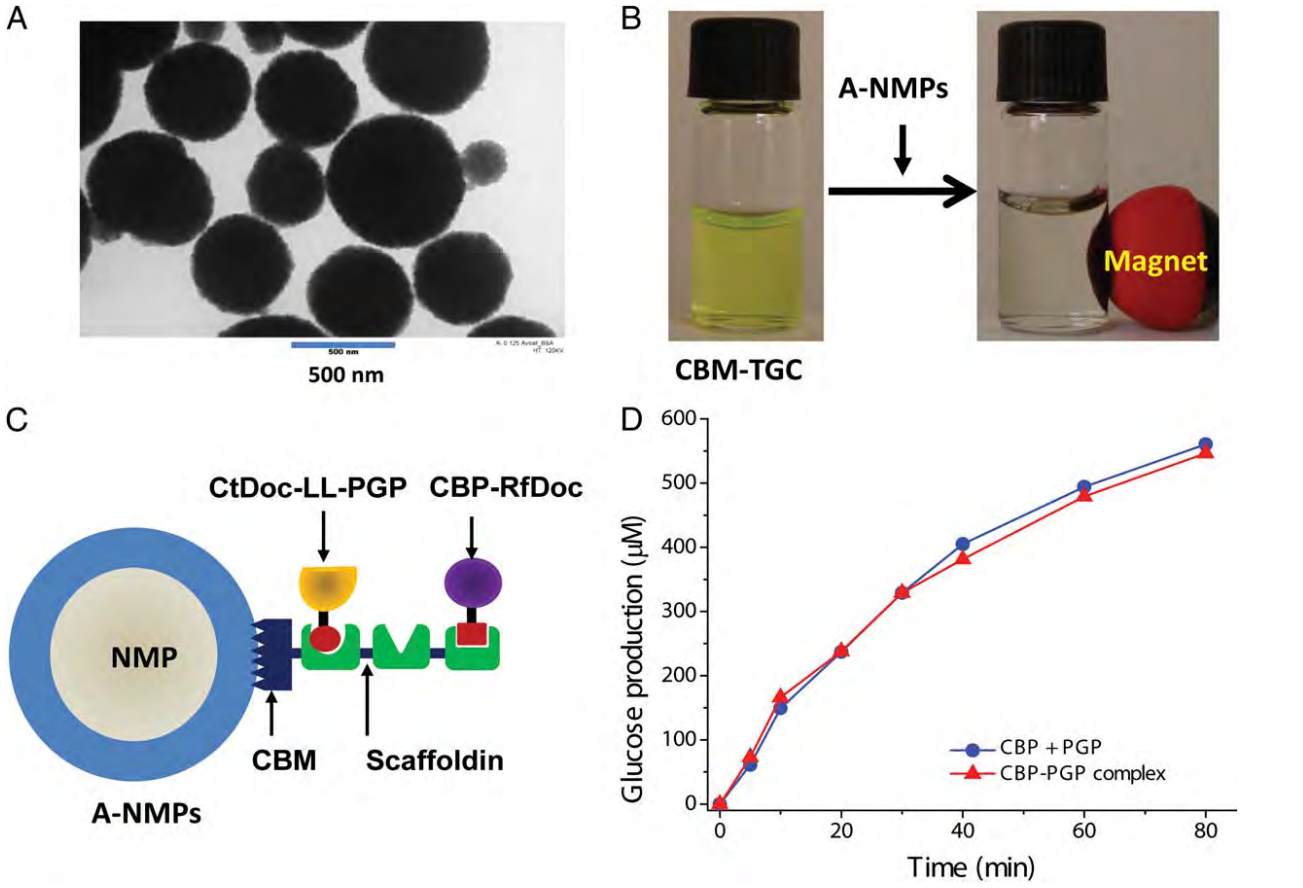

Fig. 4. Transmission electron microscopic image of Avicel-containing nanomagnetic particles (A-NMPs) (*A*), photos of A-NMPs that bind with a CBM3-tagged green fluorescent protein under magnet (*B*), the scheme of coimmobilized PGP and CBP on the A-NMPs (*C*), and starch synthesis rate comparison based on glucose formation between the coimmobilized PGP–CBP and the noncomplexed PGP and CBP mixture (*D*).

Saccharomyces cerevisiae; the yeast can produce ethanol and single-cell proteins because the yeast cannot use cellobiose and G-1-P (40, 41); a mixture of 75 μM maltodextrins with a dextrose equivalent of 16.5–19.5 was used for the primer for amylose synthesis. Under the applied conditions, the amylose yields were 25%, 23%, and 2% for RAC, COLISF-pretreated corn stover, and DA-pretreated corn stover at hour 12, respectively (Table 2). A lower cellulose digestion yield was obtained for DA-pretreated biomass because the homemade enzyme mixtures were optimized for efficient hydrolysis of amorphous cellulose rather than of crystalline cellulose and hemicellulose- and lignin-containing biomass. We also tested two commercial fungal enzyme mixtures, gifted by Novozymes and Genencor, for the hydrolysis of pretreated biomass. Much higher cellulose hydrolysis yields were obtained but ample beta-glucosidase in the commercial cellulase mixtures rapidly converted cellobiose to glucose, resulting in very low yields of amylose. After SEBF, immobilized CBP–PGP can be recycled and ethanol can be separated by distillation; the precipitated synthetic amylose is extracted using 1 M NaOH and precipitated by neutralization for obtaining high-quality amylose. The yeast cells and the biomass residuals remained in solid pellets.

Discussion

This cellulose-to-amylose biotransformation could be scaled up by increasing the stability of CBP and PGP and decreasing their production costs in terms of cost per kilogram of enzyme (Fig. S6), because this combined cellulose-hydrolyzing and starch-synthesizing enzyme mixture did not involve any labile coenzymes [e.g., CoA and NAD(P)] (Fig. 1*A*); no glucose released from the cellulose was wasted (Fig. 1); only two more enzymes were added, and they can be reused easily by a magnetic force (Fig. 4); and no energy or costly reagents were added. When both CBP–PGP enzymes have total turnover number (TTN) values of 2.6×10^6 mol of product per mole of enzyme and their cost is 20 US dollars per kilogram of enzyme, the extra enzyme cost compared with SSF in biorefineries would be 1 cent per kilogram of amylose synthesized. When enzyme costs are lower than \$20/kg and/or TTN values are higher than 2.6×10^6, the enzyme expenditure could be decreased drastically (Fig. S6). Wild-type thermophilic CBP has an estimated TTN value of $\sim 2 \times 10^6$ at 30 °C (34), whereas more stable engineered CBP by combining directed evolution and rational design has an enhanced TTN value of $\sim 2 \times 10^7$, by a factor of ~10 (42). Wild-type PGP has an estimated TTN value of $\sim 6 \times 10^4$ at 30 °C. Via directed evolution, a PGP mutant has a nearly two orders of magnitude enhancement in TTN values, being $\sim 1.7 \times 10^6$ (43). By considering the stability of immobilized glucose isomerase (29) and other immobilized thermophilic enzymes (44), further stability improvement of CBP and PGP is expected to be achieved by more rounds of mutagenesis plus enzyme immobilization soon. Another scale-up challenge could be low-cost production of CBP and PGP. Considering the production costs of bulk enzymes such as cellulase and protease (~\$10/kg) (45) and relatively fine enzymes used for biocatalysis (~\$100/kg) (30, 46), the above economic analysis based on enzyme stability and enzyme production costs could be feasible after more research and development efforts. In partial support of this, enzyme costs in the enzymatic hydrolysis of starch are only 0.3–0.6 cents per kilogram of starch hydrolyzed (29).

The theoretical yield of amylose from cellulose through this synthetic pathway is 50%, higher than the yields that we currently obtained. The practical amylose yield could be enhanced through more cellobiose production by optimizing the cellulase mixture composition and ratio, eliminating beta-glucosidase from the commercial cellulase mixtures, optimization of CBP–PGP loading, improving PGP performance, process design (47), and biomass pretreatment conditions. For potential application, the current amylose yields (e.g., 2–30%) in biorefineries would be acceptable because no sugar is wasted and the potential market for synthetic starch as food and feed could be less than 1/10th that of biofuels and biochemicals (4, 48).

Synthetic amylose has a variety of applications from high-value to low-value products, depending on its quality and potential market sizes. Top-quality amylose can be used as a chromatographic column matrix and drug capsule material in the pharmaceutical industry. Amylose can be used to make biodegradable plastics; starch-based plastics already account for 50% of the bioplastic market (5). High-quality amylose is suitable for producing transparent and flexible low-oxygen-diffusion plastic sheets and films (6). Amylose is an important thickener, water binder, emulsion stabilizer, and gelling agent in the food industry. Food-grade amylose can be blended with cereals and processed to high-amylose tailored foods for meeting special dietary needs because high-amylose wheat, corn, and rice have a much lower glycemic load. The foods with lower glycemic loads can improve human health and lower the risk of serious noninfectious diseases (e.g., diabetes and obesity) (7, 8). Medium-quality amylose can be used as a high-density hydrogen carrier for the enzymatic production of starchy hydrogen, which could solve the challenges associated with hydrogen production, hydrogen storage, infrastructure, and safety concerns (9–11). After SEBF, low-quality amylose that is mixed with yeast cells after centrifugation can be used directly as animal feed for nonruminant animals, such as pigs and chickens, for which yeast cells are currently a supplementary protein source.

To meet the growing needs for biofuels and renewable materials, as well as food and feed, whose production requires large amounts of arable land, water, and energy, there is an urgent need to use abundant and renewable nonfood agricultural and forest residues and dedicated bioenergy crops that can grow on marginal land and require low inputs. Future biorefineries based on this technology could help address the food, biofuels, and environment trilemma; decrease the impact of growing food and feed consumption on the environment; provide more healthy food; and promote the bioeconomy. Because in vitro building blocks cannot duplicate themselves, the large-scale implementation of cellulose-to-starch in future biorefineries would not raise the questions about ethics, biosecurity, and biosafety that are often confronted by in vivo synthetic biology projects.

Materials and Methods

Chemicals and Materials. Cellobiohydrolase I (TrCel7A) and endoglucanase II (TrCel5A) from *Trichoderma* spp. were purchased from Megazyme. All other enzymes expressed in *E. coli* were purified and concentrated as described elsewhere and in *SI Materials and Methods*. Insoluble regenerated amorphous cellulose (RAC) was prepared from Avicel PH105 (FMC) using concentrated phosphoric acid. Corn stover was obtained from the National

Table 2. The yields of synthetic amylose from various types of pretreated biomass at hour 12

Biomass type	Solid concentration, g/L	Cellulose content, %	Cellulose degraded, %	Amylose produced, g/L	Amylose yield, % (wt/wt)
RAC	20	100	77.2	3.82	24.7
COSLIF corn stover	38	45.7	49.4	1.97	23.0
DA corn stover	80	53.7	14.7	0.13	2.1

Reported values are the averages of three measurements, where the SDs were less than 10%.

Renewable Energy Laboratory. Experimental conditions for dilute sulfuric acid pretreatment and COSLIF were described previously (39).

Simultaneous Enzymatic Biotransformation and Fermentation. Simultaneous enzymatic biotransformation and fermentation was conducted under the following conditions: 100 mM Hepes buffer (pH 7.3) containing 20 g/L RAC, 38 g/L COSLIF-pretreated corn stover or 80 g/L DA-pretreated corn stover, 0.2 mg/mL BsCel5, 0.1 mg/mL CpCel48, 0.4 mg/mL commercial TrCel7A, 0.2 mg/mL A-NMPs immobilized CtCBP–PGP enzyme complex, 10 mM phosphate, 75 μM maltodextrin with a dextrose equivalent of 16.5–19.5, and yeast cells (final OD 0.5). Pretreated biomass was washed with water three times before use. Yeast cells were washed three times with PBS buffer (24 g/L NaCl, 0.6 g/L KCl, 5.4 g/L $Na_2HPO_4{\cdot}2H_2O$, and 0.84 g/L KH_2PO_4) before mixing them with other components. The reactions were carried out at 30 °C. The samples were taken at hour 12. The reactions were terminated by 5-min water boiling. After centrifugation, which removed denatured and precipitated enzymes, the supernatants were mixed with an equal volume of 100% ethanol to precipitate the synthetic starch. The precipitated starch was washed once with ethanol. The number of glucose units in the starch was measured by the phenol-sulfuric acid assay and enzymatic starch kit.

ACKNOWLEDGMENTS. This work was supported by the Biological Systems Engineering Department of Virginia Polytechnic Institute and State University and partially supported by the College of Agriculture and Life Sciences Biodesign and Bioprocessing Research Center, Shell GameChanger Program, and the Department of Energy BioEnergy Science Center (Y.-H.P.Z.). H.C. was partially supported by the China Scholarship Council.

1. Foley JA, et al. (2011) Solutions for a cultivated planet. *Nature* 478(7369):337–342.
2. Godfray HCJ, et al. (2010) Food security: The challenge of feeding 9 billion people. *Science* 327(5967):812–818.
3. The World Economic Forum Water Initiative (2011) *Water Security: The Water-Food-Energy-Climate Nexus* (Island Press, Washington, DC).
4. Zhang Y-HP (2013) Next-generation biorefineries will solve the food, biofuels and environmental trilemma in the energy-food-water nexus. *Energy Sci Eng*, 10.1002/ese3.2.
5. van Soest JJG, Vliegenthart JFG (1997) Crystallinity in starch plastics: consequences for material properties. *Trends Biotechnol* 15(6):208–213.
6. Frische R, Wollmann K, Gross-Lannert R, Schneider J, Best B (1994) US Patent 5374304. Special amyloses and their use for producing biodegradable plastics.
7. Regina A, et al. (2006) High-amylose wheat generated by RNA interference improves indices of large-bowel health in rats. *Proc Natl Acad Sci USA* 103(10):3546–3551.
8. Maki KC, et al. (2012) Resistant starch from high-amylose maize increases insulin sensitivity in overweight and obese men. *J Nutr* 142(4):717–723.
9. Zhang Y-HP, Huang W-D (2012) Constructing the electricity-carbohydrate-hydrogen cycle for a sustainability revolution. *Trends Biotechnol* 30(6):301–306.
10. Zhang Y-HP, Evans BR, Mielenz JR, Hopkins RC, Adams MWW (2007) High-yield hydrogen production from starch and water by a synthetic enzymatic pathway. *PLoS ONE* 2(5):e456.
11. Zhang Y-HP (2009) A sweet out-of-the-box solution to the hydrogen economy: Is the sugar-powered car science fiction? *Energy Environ. Sci.* 2(2):272–282.
12. Peat S, Bourne EJ, Barker SA (1948) Enzymic conversion of amylose into amylopectin. *Nature* 161(4082):127–128.
13. Lynd LR, Woods J (2011) Perspective: A new hope for Africa. *Nature* 474(7352): S20–S21.
14. Tuck CO, Pérez E, Horváth IT, Sheldon RA, Poliakoff M (2012) Valorization of biomass: Deriving more value from waste. *Science* 337(6095):695–699.
15. Somerville C, Youngs H, Taylor C, Davis SC, Long SP (2010) Feedstocks for lignocellulosic biofuels. *Science* 329(5993):790–792.
16. Sheppard AW, Gillespie I, Hirsch M, Begley C (2011) Biosecurity and sustainability within the growing global bioeconomy. *Curr. Opin. Environ. Sustain.* 3(1–2):4–10.
17. French CE (2009) Synthetic biology and biomass conversion: A match made in heaven? *J R Soc Interface* 6(Suppl 4):S547–S558.
18. Casillas CE, Kammen DM (2010) Environment and development. The energy-poverty-climate nexus. *Science* 330(6008):1181–1182.
19. Desvaux M, Guedon E, Petitdemange H (2001) Carbon flux distribution and kinetics of cellulose fermentation in steady-state continuous cultures of *Clostridium cellulolyticum* on a chemically defined medium. *J Bacteriol* 183(1):119–130.
20. Matheron C, Delort A-M, Gaudet G, Forano E, Liptaj T (1998) ^{13}C and ^{1}H nuclear magnetic resonance study of glycogen futile cycling in strains of the genus *Fibrobacter*. *Appl Environ Microbiol* 64(1):74–81.
21. Lynd LR, et al. (2008) How biotech can transform biofuels. *Nat Biotechnol* 26(2): 169–172.
22. Berg JM, Tymoczko JL, Stryer L (2002) *Biochemistry* (Freeman, New York), 5th Ed.
23. Wang Y, Huang W, Sathitsuksanoh N, Zhu Z, Zhang Y-HP (2011) Biohydrogenation from biomass sugar mediated by *in vitro* synthetic enzymatic pathways. *Chem Biol* 18(3):372–380.
24. Xu Y, et al. (2011) Chemoenzymatic synthesis of homogeneous ultralow molecular weight heparins. *Science* 334(6055):498–501.
25. Bujara M, Schümperli M, Pellaux R, Heinemann M, Panke S (2011) Optimization of a blueprint for *in vitro* glycolysis by metabolic real-time analysis. *Nat Chem Biol* 7(5): 271–277.
26. Swartz JR (2011) Transforming biochemical engineering with cell-free biology. *AIChE J* 58(1):5–13.
27. Guterl J-K, et al. (2012) Cell-free metabolic engineering: Production of chemicals by minimized reaction cascades. *ChemSusChem* 5(11):2165–2172.
28. Zhang Y-HP, Sun J-B, Zhong J-J (2010) Biofuel production by in vitro synthetic enzymatic pathway biotransformation. *Curr Opin Biotechnol* 21(5):663–669.
29. Zhang Y-HP (2010) Production of biocommodities and bioelectricity by cell-free synthetic enzymatic pathway biotransformations: Challenges and opportunities. *Biotechnol Bioeng* 105(4):663–677.
30. You C, Zhang Y-HP (2013) Cell-free biosystems for biomanufacturing. *Adv Biochem Eng Biotechnol* 131:89–119.
31. del Campo JSM, et al. (2013) High-yield dihydrogen production from xylose through cell-free synthetic cascade enzymes. *Angew Chem Int Ed Engl*, 10.1002/anie.201300766.
32. You C, Zhang X-Z, Sathitsuksanoh N, Lynd LR, Zhang Y-HP (2012) Enhanced microbial utilization of recalcitrant cellulose by an ex vivo cellulosome-microbe complex. *Appl Environ Microbiol* 78(5):1437–1444.
33. Ye X, et al. (2009) Spontaneous high-yield production of hydrogen from cellulosic materials and water catalyzed by enzyme cocktails. *ChemSusChem* 2(2):149–152.
34. Tanaka K, Kawaguchi T, Imada Y, Ooi T, Arai M (1995) Purification and properties of cellobiose phosphorylase from *Clostridium thermocellum*. *J Ferment Bioeng* 79(3): 212–216.
35. Ye X, Rollin J, Zhang Y-HP (2010) Thermophilic α-glucan phosphorylase from *Clostridium thermocellum*: Cloning, Characterization and Enhanced thermostability. *J Mol Catal, B Enzym* 65:110–116.
36. Ohdan K, Fujii K, Yanase M, Takaha T, Kuriki T (2007) Phosphorylase coupling as a tool to convert cellobiose into amylose. *J Biotechnol* 127(3):496–502.
37. Deng H, et al. (2005) Monodisperse magnetic single-crystal ferrite microspheres. *Angew Chem Int Ed Engl* 117(18):2842–2845.
38. You C, Myung S, Zhang Y-HP (2012) Facilitated substrate channeling in a self-assembled trifunctional enzyme complex. *Angew Chem Int Ed Engl* 51(35):8787–8790.
39. Rollin JA, Zhu Z, Sathitsuksanoh N, Zhang Y-HP (2011) Increasing cellulose accessibility is more important than removing lignin: A comparison of cellulose solvent-based lignocellulose fractionation and soaking in aqueous ammonia. *Biotechnol Bioeng* 108(1):22–30.
40. De Winter K, Cerdobbel A, Soetaert W, Desmet T (2011) Operational stability of immobilized sucrose phosphorylase: Continuous production of α-glucose-1-phosphate at elevated temperatures. *Process Biochem* 46(10):2074–2078.
41. Galazka JM, et al. (2010) Cellodextrin transport in yeast for improved biofuel production. *Science* 330(6000):84–86.
42. Ye X, Zhang C, Zhang Y-HP (2012) Engineering a large protein by combined rational and random approaches: Stabilizing the *Clostridium thermocellum* cellobiose phosphorylase. *Mol Biosyst* 8(6):1815–1823.
43. Yanase M, Takata H, Fujii K, Takaha T, Kuriki T (2005) Cumulative effect of amino acid replacements results in enhanced thermostability of potato type L α-glucan phosphorylase. *Appl Environ Microbiol* 71(9):5433–5439.
44. Myung S, Zhang X-Z, Percival Zhang YH (2011) Ultra-stable phosphoglucose isomerase through immobilization of cellulose-binding module-tagged thermophilic enzyme on low-cost high-capacity cellulosic adsorbent. *Biotechnol Prog* 27:969–975.
45. Klein-Marcuschamer D, Oleskowicz-Popiel P, Simmons BA, Blanch HW (2012) The challenge of enzyme cost in the production of lignocellulosic biofuels. *Biotechnol Bioeng* 109(4):1083–1087.
46. Tufvesson P, Lima-Ramos J, Nordblad M, Woodley JM (2011) Guidelines and cost analysis for catalyst production in biocatalytic processes. *Org Process Res Dev* 15(1): 266–274.
47. Vanderghem C, Boquel P, Blecker C, Paquot M (2010) A multistage process to enhance cellobiose production from cellulosic materials. *Appl Biochem Biotechnol* 160(8): 2300–2307.
48. MacKay DJC (2009) *Sustainable Energy–Without the Hot Air* (UIT Cambridge, Cambridge, UK).